
Learning binary or real-valued time-series via spike-timing dependent plasticity

Takayuki Osogami
IBM Research - Tokyo
osogami@jp.ibm.com

Abstract

A dynamic Boltzmann machine (DyBM) has been proposed as a model of a spiking neural network, and its learning rule of maximizing the log-likelihood of given time-series has been shown to exhibit key properties of spike-timing dependent plasticity (STDP), which had been postulated and experimentally confirmed in the field of neuroscience as a learning rule that refines the Hebbian rule. Here, we relax some of the constraints in the DyBM in a way that it becomes more suitable for computation and learning. We show that learning the DyBM can be considered as logistic regression for binary-valued time-series. We also show how the DyBM can learn real-valued data in the form of a Gaussian DyBM and discuss its relation to the vector autoregressive (VAR) model. The Gaussian DyBM extends the VAR by using additional explanatory variables, which correspond to the eligibility traces of the DyBM and capture long term dependency of the time-series. Numerical experiments show that the Gaussian DyBM significantly improves the predictive accuracy over VAR.

1 Introduction

The dynamic Boltzmann machine (DyBM) [14, 15] has recently been proposed as a model of a spiking neural network whose learning rule that maximizes the log likelihood of given *time-series* exhibits key properties of spike-timing dependent plasticity (STDP). In STDP, the amount of the change in the synaptic strength between two neurons that fired together depends on the precise timings when the two neurons fired. STDP supplements the Hebbian rule [8] and has been experimentally confirmed in biological neural networks [4]. Although the basic capability of the DyBM in learning time-series has been demonstrated in [15], its application has been limited to relatively simple tasks with low dimensional and binary-valued time-series data.

Here, we relax some of the constraints that the DyBM has required in [14, 15] in a way that it becomes more suitable for computation and learning. The primary purpose of these constraints in [14, 15] was to mimic a particular form of STDP. Our relaxed DyBM generalizes the original DyBM and allows us to interpret it as a form of logistic regression for time-series data.

We also discuss how the DyBM can deal with real-valued time-series in the form of a Gaussian DyBM, which is analogous to how Gaussian Boltzmann machines [11, 17, 9] deal with real-valued patterns as opposed to Boltzmann machines [1, 10] for binary values. Our Gaussian DyBM can be related to a vector autoregressive (VAR) model. Specifically, we show that a special case of the Gaussian DyBM is a VAR model having additional variables that capture long term dependency of time-series. These additional variables correspond to DyBM's eligibility traces, which represent how recently and frequently spikes arrived from a neuron to another.

In addition, we demonstrate the effectiveness of the Gaussian DyBM through numerical experiments. We train the Gaussian DyBM and let it predict the future values of the time-series in a purely

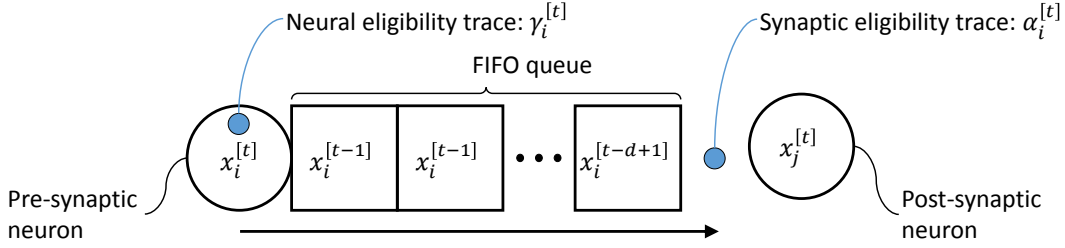


Figure 1: A connection from a (pre-synaptic) neuron i to a (post-synaptic) neuron j in a DyBM.

online manner with a stochastic gradient method [7]. Namely, at each moment, we update the parameters and the variables of the Gaussian DyBM by using only the latest values of the time-series, and let the DyBM predict the next values of time-series. The Gaussian DyBM can also be trained in a distributed manner in that each parameter can be updated using only the information that is locally available around the unit associated with that parameter. The experimental results show that the Gaussian DyBM can reduce the predictive error by up to 20 % against the corresponding VAR without noticeably increasing computational cost.

The primary contribution of this paper is in the way that we relax the constraints in the original DyBM. This relaxation allows us to represent the energy of the DyBM in a simple expression with matrices and vectors. Because the form of the energy completely determines the dynamics of the DyBM, our expression allows us to understand how the DyBM, a model of a spiking neural network, learns binary-valued time-series in a form of logistic regression. The relaxation also allows us to relate the Gaussian DyBM to VAR.

1.1 Related work

There has been a significant amount of the prior work towards understanding STDP from the perspectives of machine learning [12, 3, 16]. For example, Nessler et al. show that STDP can be understood as approximating the expectation maximization (EM) algorithm [12]. Nessler et al. study a particularly structured (winner-take-all) network and its learning rule for maximizing the log likelihood of given static patterns. On the other hand, the DyBM and the Gaussian DyBM do not assume particular structures in the network, and the learning rule having the properties of STDP applies for any synapse in the network. Also, the learning rule of the DyBM and the Gaussian DyBM maximizes the log likelihood of given time-series, and its learning rule does not involve approximations beyond what is assumed in stochastic gradient methods.

2 Extending the dynamic Boltzmann machine

We start by reviewing the DyBM as well as its learning rule that exhibits the key properties of STDP. We then relax some of the constraints of the DyBM so that it has more flexibility in performing computation and learning time-series in a form of logistic regression.

2.1 The dynamic Boltzmann machine

A DyBM is an abstract model of a spiking neural network, where a (pre-synaptic) neuron is connected to a (post-synaptic) neuron via a first-in-first-out (FIFO) queue and a synapse (see Figure 2.1). At each discrete time t , a neuron i either fires ($x_i^{[t]} = 1$) or not ($x_i^{[t]} = 0$). The spike travels along the FIFO queue and reaches the synapse after conduction delay¹, d . In other words, the FIFO queue has the length of $d - 1$ and stores, at time t , the spikes that have been generated by the pre-synaptic neuron from time $t - d + 1$ to time $t - 1$.

¹For simplicity, we assume that the conduction delay is uniform for all connections, as opposed to variable conduction delay in [15]. See also [6, 13] for ways to tune the values of the conduction delay.

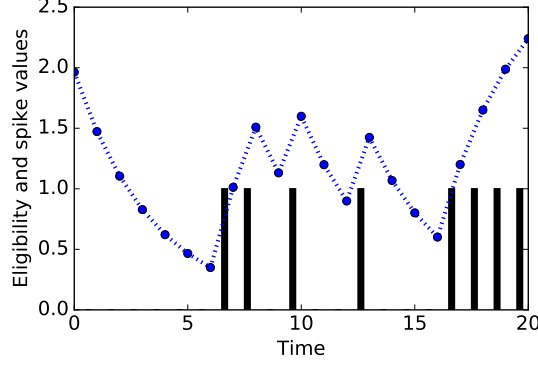


Figure 2: The value of a synaptic or neural eligibility trace as a function of time. For a synaptic eligibility trace at a synapse, the bars represent the spikes arrived from a FIFO queue at that synapse. For a neural eligibility trace at a neuron, the bars represent the spikes generated by that neuron.

Each synapse in a DyBM stores a quantity called a synaptic eligibility trace². The value of the synaptic eligibility increases when a spike arrives at the synapse from the FIFO queue; otherwise, it is decreased by a constant factor. Specifically, at time t , the value of the synaptic eligibility trace, $\alpha_i^{[t]}$, that is stored at the synapse from a pre-synaptic neuron i is updated as follows:

$$\alpha_i^{[t]} = \lambda (\alpha_i^{[t-1]} + x_i^{[t-d+1]}), \quad (1)$$

where λ is a decay rate and satisfies $0 \leq \lambda < 1$. Figure 2.1 shows an example of how the value of the synaptic eligibility trace changes depending on the spikes arrived at the synapse. Observe that $\alpha_i^{[t]}$ represents how recently and frequently spikes arrived from a pre-synaptic neuron i and can be represented non-recursively as follows:

$$\alpha_i^{[t-1]} = \sum_{s=-\infty}^{t-d} \lambda^{t-s-d} x_i^{[s]}. \quad (2)$$

Each neuron in a DyBM stores a quantity called a neural eligibility trace³. The value of the neural eligibility increases when the neuron fires; otherwise, it is decreased by a constant factor. Specifically, at time t , the value of the neural eligibility trace, $\gamma_i^{[t]}$, at a neuron i is updated as follows:

$$\gamma_i^{[t]} = \mu (\gamma_i^{[t-1]} + x_i^{[t]}), \quad (3)$$

where μ is a decay rate and satisfies $0 \leq \mu < 1$. Observe that $\gamma_i^{[t]}$ represents how recently and frequently the neuron i has fired and can be represented non-recursively as follows:

$$\gamma_i^{[t-1]} = \sum_{s=-\infty}^{t-1} \mu^{t-s} x_j^{[s]} \quad (4)$$

A neuron in a DyBM fires according to the probability distribution that depends on the energy of the DyBM. A neuron is more likely to fire when the energy becomes lower if it fires than otherwise. Let $E_j(x_j^{[t]} | \mathbf{x}^{[:t-1]})$ be the energy associated with a neuron j at time t , which can depend on whether j fires at time t (*i.e.*, $x_j^{[t]}$) as well as the preceding spiking activities of the neurons in the DyBM (*i.e.*, $\mathbf{x}^{[:t-1]}$). The firing probability of a neuron j is then given by

$$P_j(x_j^{[t]} | \mathbf{x}^{[:t-1]}) = \frac{\exp(-E_j(x_j^{[t]} | \mathbf{x}^{[:t-1]}))}{\sum_{\tilde{x} \in \{0,1\}} \exp(-E_j(\tilde{x} | \mathbf{x}^{[:t-1]}))} \quad (5)$$

²For simplicity, we assume a single synaptic eligibility trace, as opposed to multiple ones in [15], at each synapse.

³We assume a single neural eligibility trace, as opposed to multiple ones in [15], at each neuron.

for $x_j^{[t]} \in \{0, 1\}$. Specifically, $E_j(x_j^{[t]} | \mathbf{x}^{[:t-1]})$ can be represented as follows:

$$E_j(x_j^{[t]} | \mathbf{x}^{[:t-1]}) = -b_j x_j^{[t]} + E_j^{\text{LTP}}(x_j^{[t]} | \mathbf{x}^{[:t-1]}) + E_j^{\text{LTD}}(x_j^{[t]} | \mathbf{x}^{[:t-1]}), \quad (6)$$

where b_j is the bias parameter of a neuron j and represents how likely j spikes (j is more likely to fire if b_j has a large positive value), and we define

$$E_j^{\text{LTP}}(x_j^{[t]} | \mathbf{x}^{[:t-1]}) \equiv - \sum_i u_{i,j} \alpha_i^{[t-1]} x_j^{[t]} \quad (7)$$

$$E_j^{\text{LTD}}(x_j^{[t]} | \mathbf{x}^{[:t-1]}) \equiv \sum_i v_{i,j} \beta_i^{[t-1]} x_j^{[t]} + \sum_k v_{j,k} \gamma_k^{[t-1]} x_j^{[t]}, \quad (8)$$

where $\beta_i^{[t-1]}$ represents how soon and frequently spikes will arrive at the synapse from the FIFO queues from i to j :

$$\beta_i^{[t-1]} \equiv \sum_{s=t-d+1}^{t-1} \mu^{s-t} x_i^{[s]}. \quad (9)$$

In (7), the summation with respect to i is over all of the pre-synaptic neurons that are connected to j . Here, $u_{i,j}$ is the weight parameter from i to j and represents the strength of Long Term Potentiation (LTP). This weight parameter is thus referred to as LTP weight. A neuron j is more likely to fire ($x_j^{[t]} = 1$) when $\alpha_i^{[t-1]}$ is large for a pre-synaptic neuron i connected to j (spikes have recently arrived at j from i) and the corresponding $u_{i,j}$ is positive and large (LTP from i to j is strong).

In (8), the summation with respect to i is over all of the pre-synaptic neurons that are connected to j , and the summation with respect to k is over all of the post-synaptic neurons which j is connected to. Here, $v_{i,j}$ represents the strength of Long Term Depression from i to j and referred to as LTD weight. The neuron j is less likely to fire when β_i is large for a pre-synaptic neuron i connected to j (spikes will soon and frequently reach j from i) and the corresponding $v_{i,j}$ is positive and large (LTD from i to j is strong). The second term in (8) represents that a pre-synaptic neuron j is less likely to fire if a post-synaptic neuron has recently and frequently fired (γ_k is large), and the strength of this LTD is given by $v_{j,k}$. Notice that the timing of a spike is measured with respect to when the spike reaches synapse, where the spike from a pre-synaptic neuron has the delay d , and the spike from a post-synaptic neuron reaches immediately.

The learning rule of the DyBM has been derived in a way that it maximizes the log likelihood of given time-series with respect to the probability distribution given by (5) [15]. Specifically, at time t , the DyBM updates its (plastic) parameters according to

$$b_j \leftarrow b_j + \eta (x_j^{[t]} - \langle X_j^{[t]} \rangle) \quad (10)$$

$$u_{i,j} \leftarrow u_{i,j} + \eta \alpha_i^{[t-1]} (x_j^{[t]} - \langle X_j^{[t]} \rangle) \quad (11)$$

$$v_{i,j} \leftarrow v_{i,j} + \eta \beta_i^{[t-1]} (\langle X_j^{[t]} \rangle - x_j^{[t]}) + \eta \gamma_j^{[t-1]} (\langle X_i^{[t]} \rangle - x_i^{[t]}) \quad (12)$$

for each of neurons i and j , where η is a learning rate, $x_j^{[t]}$ is the training data given to j at time t , and $\langle X_j^{[t]} \rangle$ denotes the expected value of $x_j^{[t]}$ (i.e., firing probability of a neuron j at time t) according to the probability distribution given by (5).

In (10), b_j is increased when $x_j^{[t]} = 1$ is given to j , so that j becomes more likely to fire (in accordance with the training data), but the amount of the change in b_j is small if j is already likely to fire ($\langle X_j^{[t]} \rangle \approx 1$). This dependency on $\langle X_j^{[t]} \rangle$ can be considered as a form of homeostatic plasticity.

In (11), $u_{i,j}$ is increased (LTP gets stronger) when $x_j^{[t]} = 1$ is given to j . Then j becomes more likely to fire when spikes from i have recently and frequently arrived at j (i.e., $\alpha_i^{[t-1]}$ is large). This amount of the change in $u_{i,j}$ depends on $\alpha_i^{[t-1]}$, exhibiting a key property of STDP. In particular, $u_{i,j}$ is increased by a large amount if spikes from i have recently and frequently arrived at j .

According to the second term on the right-hand side of (12), $v_{i,j}$ is increased (LTD gets stronger) when $x_j^{[t]} = 0$ is given to a post-synaptic neuron j . Then j becomes less likely to fire when spikes

from i are expected to reach j soon (*i.e.*, $\beta_i^{[1]}$ is large). This amount of the change in $v_{i,j}$ is large if there are spikes in the FIFO queue from i to j and they are close to j . According to the last term of (12), $v_{i,j}$ is increased when $x_i^{[t]} = 0$ is given to the pre-synaptic i , and this amount of the change in $v_{i,j}$ is proportional to γ_j (*i.e.*, how frequently and recently the post-synaptic j has fired). This learning rule of (12) thus exhibits some of the key properties of LTD with STDP.

2.2 Giving flexibility to the DyBM

It has been shown in [15] that the DyBM in Section 2.1 has the capability of associative memory and anomaly detection for sequential patterns, but the applications of the DyBM has been limited to simple tasks with relatively low dimensional time-series. Here, we relax some of the constraints of this DyBM in a way that it gives more flexibility that is useful for learning and inference.

Specifically, observe that the first term on the right-hand side of (8) can be rewritten with the definition of $\beta_i^{[t-1]}$ in (9) as follows:

$$\sum_i v_{i,j} \beta_i^{[t-1]} x_j^{[t]} = \sum_i \sum_{s=t-d+1}^{t-1} v_{i,j} \mu^{s-t} x_i^{[s]} x_j^{[t]} \quad (13)$$

$$= \sum_i \sum_{\delta=1}^{d-1} v_{i,j}^{[\delta]} x_i^{[t-\delta]} x_j^{[t]}, \quad (14)$$

where we let $v_{i,j}^{[\delta]} \equiv v_{i,j} \mu^{-\delta}$. Here, $v_{i,j}^{[\delta]}$ represents how unlikely j fires at time t if i fired at time $t - \delta$. The parametric form of $v_{i,j}^{[\delta]} \equiv v_{i,j} \mu^{-\delta}$ assumes that this LTD weight decays geometrically as the interval, δ , between the two spikes increases.

In the following, we relax this constraint on $v_{i,j}^{[\delta]}$ for $\delta = 1, \dots, d-1$ and assumes that these LTD weights can take independent values. Then the energy of the DyBM with N neurons can be represented conveniently with matrix and vector operations:

$$E(\mathbf{x}^{[t]} | \mathbf{x}^{[:t-1]}) \equiv \sum_{j=1}^N E_j(x_j^{[t]} | \mathbf{x}^{[:t-1]}) \quad (15)$$

$$= -\mathbf{b}^\top \mathbf{x}^{[t]} - (\boldsymbol{\alpha}_\lambda^{[t-1]})^\top \mathbf{U} \mathbf{x}^{[t]} + \sum_{\delta=1}^{d-1} (\mathbf{x}^{[t-\delta]})^\top \mathbf{V}^{[\delta]} \mathbf{x}^{[t]} + (\mathbf{x}^{[t]})^\top \mathbf{V} \boldsymbol{\gamma}_\mu^{[t-1]}, \quad (16)$$

where $\mathbf{b} \equiv (b_j)_{j=1, \dots, N}$ is a vector, $\mathbf{U} \equiv (u_{i,j})_{(i,j) \in \{1, \dots, N\}^2}$ is a matrix, and other boldface letters are defined analogously (a vector is lowercase and a matrix is uppercase). For eligibility traces ($\boldsymbol{\alpha}_\lambda^{[t-1]}$ and $\boldsymbol{\gamma}_\mu^{[t-1]}$), we append the subscript to explicitly represent the dependency on the decay rate (λ and μ). The functional form of the energy completely determines the dynamics of a DyBM, and relaxing its constraints allows the DyBM to represent a wider class of dynamical systems.

Notice that the last term of (16) can be divided into two terms:

$$(\mathbf{x}^{[t]})^\top \mathbf{V} \boldsymbol{\gamma}_\mu^{[t-1]} = (\boldsymbol{\gamma}_\mu^{[t-1]})^\top \mathbf{V} \mathbf{x}^{[t]} \quad (17)$$

$$= (\boldsymbol{\alpha}_\mu^{[t-1]})^\top \mathbf{V} \mathbf{x}^{[t]} + \sum_{\delta=1}^{d-1} (\mathbf{x}^{[t-\delta]})^\top \hat{\mathbf{V}}^{[\delta]} \mathbf{x}^{[t]}, \quad (18)$$

where $\boldsymbol{\alpha}_\mu^{[t-1]}$ is the same as the vector of synaptic eligibility traces but with the decay rate μ , and $\hat{\mathbf{V}}^{[\delta]} \equiv \mu^{-\delta} \mathbf{V}$. Comparing (18) and (16), we find that, without loss of generality, the energy of the DyBM can be represented with the following form:

$$E(\mathbf{x}^{[t]} | \mathbf{x}^{[:t-1]}) = -\left(\mathbf{b}^\top + \sum_{\delta=1}^{d-1} (\mathbf{x}^{[t-\delta]})^\top \mathbf{W}^{[\delta]} + \sum_{\ell=1}^L (\boldsymbol{\alpha}_{\lambda_\ell}^{[t-1]})^\top \mathbf{U}_\ell \right) \mathbf{x}^{[t]}, \quad (19)$$

where we define $\mathbf{W}^{[\delta]} = -\mathbf{V}^{[\delta]} - \hat{\mathbf{V}}^{[\delta]}$. The energy in (19) reduces to the original energy in (6) when $\mathbf{W}^{[\delta]} = -\mu^{-\delta} \mathbf{V} - \mu^\delta \mathbf{V}^\top$, $\mathbf{U}_1 = \mathbf{U}$, $\mathbf{U}_2 = -\mu^d \mathbf{V}^\top$, $\lambda_1 = \lambda$, $\lambda_2 = \mu$, and $L = 2$. With

$L > 2$, one can also incorporate multiple synaptic or neural eligibility traces with varying decay rates in [15]. Equivalently, we can represent the energy using neural eligibility traces, γ_{μ_ℓ} , instead of synaptic eligibility traces, α_{λ_ℓ} , as follows:

$$E(\mathbf{x}^{[t]}|\mathbf{x}^{[:t-1]}) = -\left(\mathbf{b}^\top + \sum_{\delta=1}^{d-1}(\mathbf{x}^{[t-\delta]})^\top \mathbf{W}^{[\delta]} + \sum_{\ell=1}^L(\gamma_{\mu_\ell}^{[t-1]})^\top \mathbf{V}_\ell\right) \mathbf{x}^{[t]}. \quad (20)$$

2.3 Logistic regression for time-series with the DyBM

We now show that we are actually learning a kind of a logit model for time-series by learning a DyBM. Let

$$\mathbf{m}^{[t]} \equiv \mathbf{b}^\top + \sum_{\delta=1}^{d-1}(\mathbf{x}^{[t-\delta]})^\top \mathbf{W}^{[\delta]} + \sum_{\ell=1}^L(\alpha_{\lambda_\ell}^{[t-1]})^\top \mathbf{U}_\ell. \quad (21)$$

Then we can write (6) as $E_j(x_j^{[t]}|\mathbf{x}^{[:t-1]}) = -m_j^{[t]} x_j^{[t]}$.

The firing probability in (6) can now be expressed as

$$P_j(x_j^{[t]}|\mathbf{x}^{[:t-1]}) = \frac{\exp(m_j^{[t]} x_j^{[t]})}{1 + \exp(m_j^{[t]})} \quad (22)$$

for $x_j^{[t]} \in \{0, 1\}$. Namely, $m_j^{[t]}$ represents the negative energy associated with a neuron j on the condition that j fires at time t , and j is likely to fire at t if $m_j^{[t]}$ is positive and large. Recall that $m_j^{[t]}$ depends on $\mathbf{x}^{[:t-1]}$.

The form of (22) implies that the DyBM is a kind of a logit model, where the feature vector, $(\mathbf{x}^{[t-d+1]}, \dots, \mathbf{x}^{[t-1]}, \alpha_{\lambda}^{[t-1]}, \alpha_{\mu}^{[t-1]})$, depends on the prior values, $\mathbf{x}^{[:t-1]}$, of the time-series. By applying the learning rules given in (10)-(12) to given time-series, we can learn the parameters of the DyBM or equivalently the parameters of the logit model (*i.e.*, \mathbf{b} , $\mathbf{W}^{[\delta]}$ for $\delta = 1, \dots, d-1$, and \mathbf{U}_ℓ for $\ell = 1, \dots, L$) in (22).

3 Gaussian dynamic Boltzmann machines

In this section, we show how a DyBM can deal with real-valued time-series in the form of a Gaussian DyBM. A Gaussian DyBM assumes that $x_j^{[t]}$ follows a Gaussian distribution for each j :

$$p_j(x_j^{[t]}|\mathbf{x}^{[t-T, t-1]}) = \frac{1}{\sqrt{2\pi\sigma_j^2}} \exp\left(-\frac{(x_j^{[t]} - m_j^{[t]})^2}{2\sigma_j^2}\right), \quad (23)$$

where $m_j^{[t]}$ is given by (21), and σ_j^2 is a variance parameter. This Gaussian distribution is in contrast to the Bernoulli distribution of the DyBM given by (5).

We now derive a learning rule for the Gaussian DyBM in a way that it maximizes the log-likelihood of given time-series $\mathbf{x}^{[1]}$:

$$\sum_t \log p(\mathbf{x}^{[t]}|\mathbf{x}^{[:t-1]}) = \sum_t \sum_{i=1}^N \log p_i(x_i^{[t]}|\mathbf{x}^{[-\infty, t-1]}), \quad (24)$$

where the summation over t is over all of the time steps of $\mathbf{x}^{[1]}$, and the conditional independence between $x_i^{[t]}$ and $x_j^{[t]}$ for $i \neq j$ given $\mathbf{x}^{[:t-1]}$ is the fundamental property of the DyBM shown in [15].

The approach of stochastic gradient is to update the parameters of the Gaussian DyBM at each step, t , according to the gradient of the conditional probability density of $\mathbf{x}^{[t]}$:

$$\nabla \log p(\mathbf{x}^{[t]}|\mathbf{x}^{[:t-1]}) = -\sum_{i=1}^N \left(\frac{1}{2} \nabla \log \sigma_i^2 + \nabla \frac{(x_i^{[t]} - m_i^{[t]})^2}{2\sigma_i^2}\right), \quad (25)$$

where the equality follow from (23). From (25) and (21), we can derive the derivative with respect to each parameter.

These parameters are thus updated as follows⁴:

$$b_j \leftarrow b_j + \eta \frac{x_j^{[t]} - m_j^{[t]}}{\sigma_j^2}, \quad \sigma_j \leftarrow \sigma_j + \eta \left(\frac{(x_j^{[t]} - m_j^{[t]})^2}{\sigma_j^2} - 1 \right) \frac{1}{\sigma_j}, \quad (26)$$

$$w_{i,j}^{[\delta]} \leftarrow w_{i,j}^{[\delta]} + \eta \frac{x_j^{[t]} - m_j^{[t]}}{\sigma_j^2} x_i^{[t-\delta]}, \quad u_{i,j,\ell} \leftarrow u_{i,j,\ell} + \eta \frac{x_j^{[t]} - m_j^{[t]}}{\sigma_j^2} \alpha_{i,\lambda_\ell}^{[t-1]} \quad (27)$$

for $\ell = 1, \dots, L$, $\delta = 1, \dots, d-1$, and $(i, j) \in \{1, \dots, N\}^2$, where η is the learning rate. In (26)-(27), $m_j^{[t]}$ is given by (21), $u_{i,j,\ell}$ is the (i, j) element of \mathbf{U}_ℓ , and α_{i,λ_ℓ} is the i -th element of $\boldsymbol{\alpha}_{\lambda_\ell}$.

The maximum likelihood estimator of $\mathbf{x}^{[t]}$ by the Gaussian DyBM is given by $\mathbf{m}^{[t]}$ in (21). The Gaussian DyBM can thus be understood as a modification to the standard VAR. Specifically, the last term in the right-hand side of (21) involves eligibility traces, which can be understood as features of historical values, $\mathbf{x}^{[t-d]}$, and are added as new variables of the VAR model. Because the value of the eligibility traces can depend on the infinite past, the Gaussian DyBM can take into account the history beyond the lag d .

4 Numerical experiments

We now demonstrate the advantages of the Gaussian DyBM through numerical experiments. The purpose of our experiment is to demonstrate the effectiveness of the eligibility traces of the Gaussian DyBM. Specifically, we train the Gaussian DyBM with a one dimensional sequence, which is generated according to the following noisy sine wave:

$$x^{[t]} = \sin(2\pi t/100) + \varepsilon^{[t]} \quad (28)$$

for each t , where $\varepsilon^{[t]}$ is independent and identically distributed with the standard Gaussian distribution. All of the experiments are carried out with a Python 2.7 implementation on a Linux machine having 32 cores of POWER8 and 64 GB memory.

We consider a Gaussian DyBM, with the representation (20), having a single unit ($N = 1$), which is connected to itself with a FIFO queue of length d and has a neural eligibility trace of decay rate μ . We vary d and μ in the experiment. This Gaussian DyBM makes a prediction, $m^{[t]}$, according to

$$m^{[t]} = b + \sum_{\delta=1}^{d-1} w^{[\delta]} x^{[t-\delta]} + v \gamma^{[t-1]}, \quad (29)$$

where $\gamma^{[t-1]} \equiv \sum_{s=1}^{\infty} \mu^{s-d} x^{[t-s]}$, and (b, w, v) is the set of parameters of the Gaussian DyBM. For $\mu = 0$, we define $\gamma^{[t-1]} = x^{[t-d]}$, and this Gaussian DyBM reduces to a VAR model with d lags.

We train the Gaussian DyBM in an online manner. Namely, for each step t , we give a pattern, $x^{[t]}$, to the Gaussian DyBM to update its eligibility trace, FIFO queue, and parameters, and then let the Gaussian DyBM predict the next pattern, $x^{[t+1]}$. This process is repeated sequentially for $t = 1, 2, \dots$. Here, the parameters are updated according to natural gradients (38)-(39). The learning rate, η , in (38)-(39) is adjusted for each parameter according to AdaGrad [7], where the initial learning rate is set $\eta = 0.001$. Throughout, the initial values of the parameters and variables, including eligibility traces and the values in the FIFO queues, are set 0 except that we initialize $\sigma_j^2 = 1$ for each j to avoid division by 0.

Figure 3 shows the predictive error of the Gaussian DyBM. Here, the prediction, $m^{[t]}$, for the pattern at time t is evaluated with mean squared error, $\text{MSE}^{[t]} \equiv \frac{1}{100} \sum_{s=t-50}^{50} (m^{[t]} - x^{[t]})^2$, and $\text{MSE}^{[t]}$ is further averaged over 100 independent runs of the experiment to make the curves in the figure

⁴In Appendix A.1, we derive learning rules based on natural gradients [2].

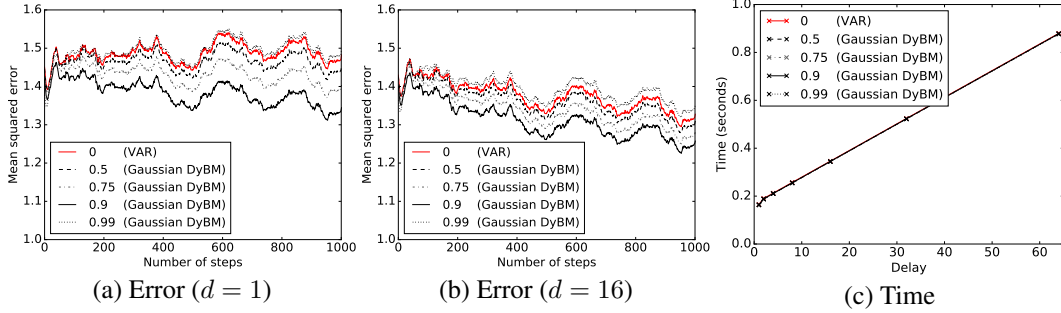


Figure 3: Squared error of prediction and learning time of Gaussian DyBMs and VAR models. (a)-(b) For each step t , the squared error is averaged over 100 independent runs. Decay rate μ is varied as in the legend, and the red curve ($\mu = 0$) corresponds to a VAR model. Conduction delay d is varied across panels. (c) The learning time per a run of 1,000 steps is plotted against delay d . Gaussian DyBMs and VAR are indistinguishable in the figure.

smooth. Due to the noise $\varepsilon^{[t]}$, the best possible squared error is 1.0 in expectation. We vary μ as indicated in the legend and d as indicated below each panel.

Although the accuracy of the prediction with the Gaussian DyBM depends on the choice of μ , the figure shows that the Gaussian DyBM (with $\mu > 0$; black curves) generally outperforms the corresponding VAR model ($\mu = 0$; red curves) and reduces the error by up to 20%. The gain that the Gaussian DyBM has over the VAR stems solely from the use of the eligibility trace, $\gamma^{[t-1]}$, instead of the lag- d variable, $x^{[t-d]}$. The results for longer conduction delay can be found in Appendix A.2.

A Gaussian DyBM performs relatively well even with $d = 1$, because, unlike VAR, history beyond $d = 1$ is taken into account in eligibility traces. The figure shows that VAR performs significantly better with $d = 16$ and becomes comparable to the Gaussian DyBM with $d = 1$. A larger d , however, comes at the expense of increased computational complexity. Here, notice that a Gaussian DyBM has essentially equivalent computational complexity as the corresponding VAR, as we use a single decay rate ($L = 1$). Figure 3(c) indeed shows that the Gaussian DyBM runs as fast as the VAR, and their learning time grows linearly with respect to the delay d . In general, for a densely connected Gaussian DyBM, per-step computational complexity is $O((L + d)N^2)$, where L is the number of decay rates, d is the maximum conduction delay, and N is the number of neurons. The computational complexity is reduced to $O((L + d)MN)$ when each neuron is connected to at most M neurons.

5 Conclusion

A DyBM is a model of a spiking neural network, and we have shown how the DyBM can be used to learn binary or real-valued time-series. For binary-valued time-series, the DyBM can be seen as logistic regression for predicting the next (spiking) pattern on the basis of the history of (spiking) patterns. The DyBM deals with real-valued time-series in the form of a Gaussian DyBM, and we have seen that the Gaussian DyBM extends a VAR model by including eligibility traces as additional explanatory variables, which allow the Gaussian DyBM to capture long term dependency of time-series. Our experimental results demonstrate the effectiveness of the eligibility traces in increasing the predictive accuracy.

The Gaussian DyBM is only one way to deal with real values by a DyBM. In particular, a DyBM may assume the distribution in the exponential family [17] instead of the Gaussian distribution. The Gaussian DyBM may also be extended to allow nonlinear hidden units. In [5], we will extend this preliminary manuscript and study a Gaussian DyBM with such extensions.

Acknowledgments

This research is supported by CREST, JST.

References

- [1] D. H. Ackley, G. E. Hinton, and T. J. Sejnowski. A learning algorithm for Boltzmann machines. *Cognitive Science*, 9:147169, 1985.
- [2] S. Amari and H. Nagaoka. *Methods of Information Geometry*. Oxford University Press, 2000.
- [3] Y. Bengio, T. Mesnard, A. Fischer, S. Zhang, and Y. Wu. STDP as presynaptic activity times rate of change of postsynaptic activity. arXiv:1509.05936v2, 2016.
- [4] G. Bi and M. Poo. Synaptic modifications in cultured hippocampal neurons: Dependence on spike timing, synaptic strength, and postsynaptic cell type. *Journal of Neuroscience*, 18:1046410472, 1998.
- [5] S. Dasgupta and T. Osogami. Nonlinear dynamic Boltzmann machines for time series prediction. In *Proceedings of the Thirty-First AAAI Conference on Artificial Intelligence (AAAI-17)*, 2017.
- [6] S. Dasgupta, T. Yoshizumi, and T. Osogami. Regularized dynamic Boltzmann machine with delay pruning for unsupervised learning of temporal sequences. In *Proceedings of the 23rd International Conference on Pattern Recognition*, 2016.
- [7] J. Duchi, E. Hazan, and Y. Singer. Adaptive subgradient methods for online learning and stochastic optimization. *Journal of Machine Learning Research*, 12:2121–2159, 2011.
- [8] D. O. Hebb. *The organization of behavior: A neuropsychological approach*. Wiley, 1949.
- [9] G. E. Hinton and R. Salakhutdinov. Reducing the dimensionality of data with neural networks. *Science*, 313:504507, 2006.
- [10] G. E. Hinton and T. J. Sejnowski. Optimal perceptual inference. In *Proc. IEEE Conference on Computer Vision and Pattern Recognition*, pages 448–453, June 1983.
- [11] T. Marks and J. Movellan. Diffusion networks, products of experts, and factor analysis. In *Proceedings of the Third International Conference on Independent Component Analysis and Blind Source Separation*, 2001.
- [12] B. Nessler, M. Pfeiffer, L. Buesing, and W. Maass. Bayesian computation emerges in generic cortical microcircuits through spike-timing-dependent plasticity. *PLoS Computational Biology*, 9(4):e1003037, 2013.
- [13] T. Osogami and S. Dasgupta. Learning the values of the hyperparameters of a dynamic Boltzmann machine. *IBM Journal of Research and Development*, 61(4/5):to appear, 2017.
- [14] T. Osogami and M. Otsuka. Learning dynamic Boltzmann machines with spike-timing dependent plasticity. Technical Report RT0967, IBM Research, 2015.
- [15] T. Osogami and M. Otsuka. Seven neurons memorizing sequences of alphabetical images via spike-timing dependent plasticity. *Scientific Reports*, 5:14149, 2015.
- [16] B. Scellier and Y. Bengio. Equilibrium propagation: Bridging the gap between energy-based models and backpropagation. arXiv:1602.05179v4, 2016.
- [17] M. Welling, M. Rosen-Zvi, and G. E. Hinton. Exponential family harmoniums with an application to information retrieval. In *Advances in Neural Information Processing Systems 17*, pages 1481–1488. MIT Press, 2004.

A Supplementary material for *Gaussian dynamic Boltzmann machines*

A.1 Natural gradients

Consider a stochastic model that gives the probability density of a pattern \mathbf{x} as $p(\mathbf{x}; \theta)$. With natural gradients [2], the parameters, θ , of the stochastic model are updated as follows:

$$\theta_{t+1} = \theta_t - \eta_t G^{-1}(\theta_t) \nabla \log p(\mathbf{x}; \theta) \quad (30)$$

at each step t , where η_t is the learning rate at t , and $G(\theta)$ denotes the Fisher information matrix:

$$G(\theta) \equiv \int p(\mathbf{x}; \theta) (\nabla \log p(\mathbf{x}; \theta) \nabla \log p(\mathbf{x}; \theta)^\top) d\mathbf{x}. \quad (31)$$

Due to the conditional independence in (24), it suffices to derive a natural gradient for each Gaussian unit. Here, we consider the parametrization with mean m and variance $v \equiv \sigma^2$. The probability density function of a Gaussian distribution is represented with this parametrization as follows:

$$p(x; m, v) = \frac{1}{\sqrt{2\pi v}} \exp\left(-\frac{(x-m)^2}{2v}\right). \quad (32)$$

The log likelihood of x is then given by

$$\log p(x; m, v) = -\frac{(x-m)^2}{2v} - \frac{1}{2} \log v - \frac{1}{2} \log 2\pi. \quad (33)$$

Hence, the gradient and the inverse Fisher information matrix in (30) are given as follows:

$$\nabla \log p(\mathbf{x}; \theta) = \left(\begin{array}{c} \frac{x-m}{v} \\ \frac{(x-m)^2}{2v^2} - \frac{1}{2v} \end{array} \right) \quad (34)$$

$$G^{-1}(\theta) = \left(\begin{array}{cc} \frac{1}{v} & 0 \\ 0 & \frac{1}{2v^2} \end{array} \right)^{-1} = \left(\begin{array}{cc} v & 0 \\ 0 & 2v^2 \end{array} \right), \quad (35)$$

The parameters $\theta_t \equiv (m_t, v_t)$ are then updated as follows:

$$m_{t+1} = m_t + \eta_t (x - m_t) \quad (36)$$

$$v_{t+1} = v_t + \eta_t ((x - m_t)^2 - v_t). \quad (37)$$

In the context of a Gaussian DyBM, the mean is given by (21), where $m_j^{[t]}$ is linear with respect to b_j , $w_{i,j}$, and $u_{i,j,\ell}$. Also, the variance is given by σ_j^2 . Hence, the natural gradient gives the learning rules for these parameters as follows:

$$b_j \leftarrow b_j + \eta (x_j^{[t]} - m_j^{[t]}), \quad \sigma_j^2 \leftarrow \sigma_j^2 + \eta ((x_j^{[t]} - m_j^{[t]})^2 - \sigma_j^2), \quad (38)$$

$$w_{i,j}^{[\delta]} \leftarrow w_{i,j}^{[\delta]} + \eta (x_j^{[t]} - m_j^{[t]}) x_i^{[t-\delta]}, \quad u_{i,j,\ell} \leftarrow u_{i,j,\ell} + \eta (x_j^{[t]} - m_j^{[t]}) \alpha_{i,\lambda_\ell}^{[t-1]}, \quad (39)$$

which can be compared against what the standard gradient gives in (26)-(27).

A.2 Additional results of experiments

Figure 4 shows additional results of the experiments shown in Figure 3. Now, the conduction delay varies from $d = 32$ to $d = 64$. Learning the noisy sine wave (28) becomes rather trivial with $d > 50$, because the expected value of the noisy sine wave with the period of 100 satisfies $E[x^{[t]}] = -E[x^{[t-50]}]$. Namely, 29 can exactly represent this noisy sine wave by setting $w^{[50]} = 1$ and other parameters zero.

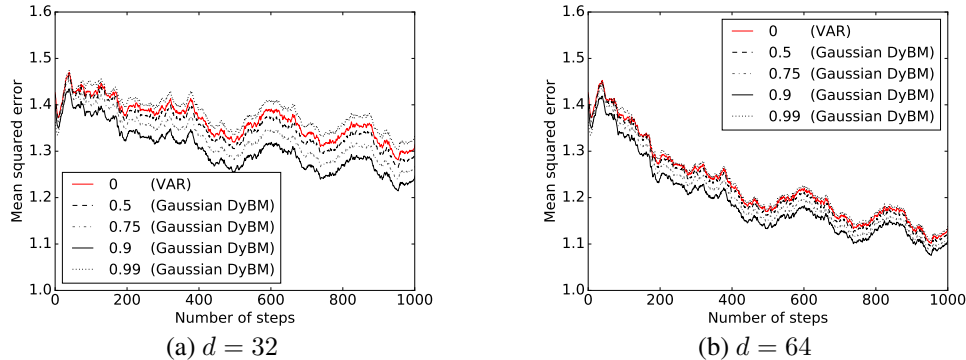


Figure 4: The results with longer conduction delay d for the experiments in Figure 3.